# The pressure variation in the electronic charge density of LiH



1989 J. Phys.: Condens. Matter 1 1601

(http://iopscience.iop.org/0953-8984/1/9/006)

J. Phys.: Condens. Matter **1** (1989) 1601–1612. Printed in the UK

# The pressure variation in the electronic charge density of LiH

C O Rodriguez†‡ and K Kunc

Laboratoire de Physique des Solides (associé au CNRS), Université P et M Curie, Tour 13, 4 place Jussieu, 75230 Paris Cédex 05, France

Received 1 July 1988, in final form 19 September 1988

**Abstract.** The behaviour under pressure of the real-space distribution of the electronic charge density of lithium hydride is determined from first principles using the density functional theory, with norm-conserving pseudopotentials and Ceperley–Alder exchange. The influence of zero-point vibrations on the ground-state properties is discussed. The integrated charge surrounding Li and H is determined quantitatively and studied as a function of pressure.

## 1. Introduction

Known to a large public as the source of negative hydrogen ions in experiments on fusion, lithium hydride (LiH) is interesting to solid state physics because it provides a prototype of extreme ionic bonding; it naturally raises the question of how far ideas pertinent to alkali halides can be extrapolated to the hydrides. Owing to its privileged position near the top of the periodic system, the electronic and certain related properties of LiH have been addressed for several decades [1, 2]. Hartree–Fock calculations of cohesive energy (for a review see, e.g., [3]) [4–7] and of the electronic band structure [8–10] have been performed. There have also been a number of theoretical and experimental studies on its equation of state [9, 11–14], elasticity [15], x-ray [16], Brillouin [17] and Raman scattering [18], phonons [19–22] and other properties [23]. In many cases, LiH was among the very first substances studied by the above methods. Judging by the efforts invested, one can see that the technical simplifications derived from the small number of electrons, which were crucial to the techniques available years ago, are largely counterbalanced by the difficulties brought about by the small and light atoms; the deep electron–ion potentials, which are difficult to deal with, and the prominent effects of the zero-point motion are consequences of the top-of-the-table position too.

Recently, the interest in LiH has been revived, mainly owing to experimental work on x-ray scattering [24, 25] and Compton profiles [26]. Very little is known, both theoretically and experimentally, on elementary characteristics, e.g. valence charge distribution [27]. It may be the success of the Born model that has accredited the idea of a perfectly ionic crystal although the doubts about the validity of this representation

† Present address: Max Planck Institut für Festkörperforschung, Heisenbergstrasse 1, D-7000 Stuttgart 80, Federal Republic of Germany.

‡ Permanent address: Instituto de Física de Líquidos y Sistemas Biológicos, Facultad de Ciencias Exactas, Universidad Nacional de La Plata, C C 565, La Plata (1900), Argentina.

0953-8984/89/091601 + 12 $02.50 

were expressed [2] as early as 1936 and, among others, the presence of a homopolar contribution to the bonding was suggested [4].

In what follows, we attempt to give a quantitative picture of the pressure variation in the real space of the distribution of the electronic charge density in LiH which we calculate within the local density approximation (LDA) [28], using norm-conserving pseudopotentials [29] and Ceperley–Alder exchange [30]. As a strong charge transfer from Li to H is found, we propose different quantitative estimates for the integrated charges on atoms and compare them with experiment. The role of zero-point vibrations in the determination of ground-state properties is discussed as well. The paper is organised as follows: the method for dealing with the electronic energy and the inclusion of zero-point vibrations are discussed in § 2, together with our results on structural properties. The electronic energy levels and the pressure dependence of charge densities are given in § 3. The results are further discussed in § 4. A short summary of the first results has been published earlier [27].

## 2. Calculation of energy: the role of zero-point vibrations

In what follows the density functional (DF) theory [28] is applied in the local density approximation (LDA) using the plane-wave basis [31], with the norm-conserving pseudopotentials [29] and the exchange–correlation by the Ceperley–Alder form [30]. Most of the results shown below were obtained with plane-wave expansions limited by a kinetic energy of 60 Ryd (about 900 waves at $a = 4.08$ Å) and the cut-offs up to 72 Ryd (about 1200 waves) were used in the tests; the plane waves beyond 48 Ryd were treated by Löwdin perturbation theory. A set of ten special $\boldsymbol{k}$-points was used for sampling the Brillouin zone, their number was increased up to 28 points in tests.

The ground-state energy $E^{\mathrm{LDA}}$ of the system of valence electrons +2 cores per unit cell, calculated as a function of lattice parameter $a$, is shown in figure 1; the external pressure $p = -\partial E/\partial V$ evaluated using the 'stress theorem' [32] is also given. It is straightforward to connect the calculated points by the Murnaghan [33] equation

$$E - E_0 = -(B_0 V_0/B_0')\{[(V/V_0)^{1-B_0'} - 1]/(1 - B_0') - (V/V_0 - 1)\} \tag{1}$$

and to determine the position of the minimum and the second and third derivatives of $E^{\mathrm{LDA}}(a)$—the quantities which, in other compounds, would be readily identified with the equilibrium lattice constant $a_0$, bulk modulus $B$ and its pressure derivative $B'$; these values are given in table 1, which illustrates convergence of the static properties with the number of plane waves and number of sampling points. It allows us to estimate the uncertainties consequent on the finite plane-wave cut-offs to be approximately 1% for $a_0$ and 8% for $B_0$ and the errors due to the limited number of special points not to exceed 0.6% and 4%, respectively. One can see also in figure 1 that with the 60 Ryd cut-off the calculation of static properties is converged because the pressure evaluated directly by the DF method (full curve) agrees well with that obtained as the derivative of the $E(a)$ curve (broken curve), thus suggesting [34] that the extreme values for the uncertainties in $a_0$ do not exceed 1%; at the present stage, we do not consider it useful to extend the precision further, in view of the still large uncertainties which influence the results for other physical reasons and which are discussed further on.

At this point, the major difficulty in assessing the static equilibrium consists in properly accounting for the effect of zero-point vibrations. At $T = 0$ the crystal's total energy consists of the energy $E^{\mathrm{LDA}}$ of the system of electrons + (static) ions (figure 1), to which

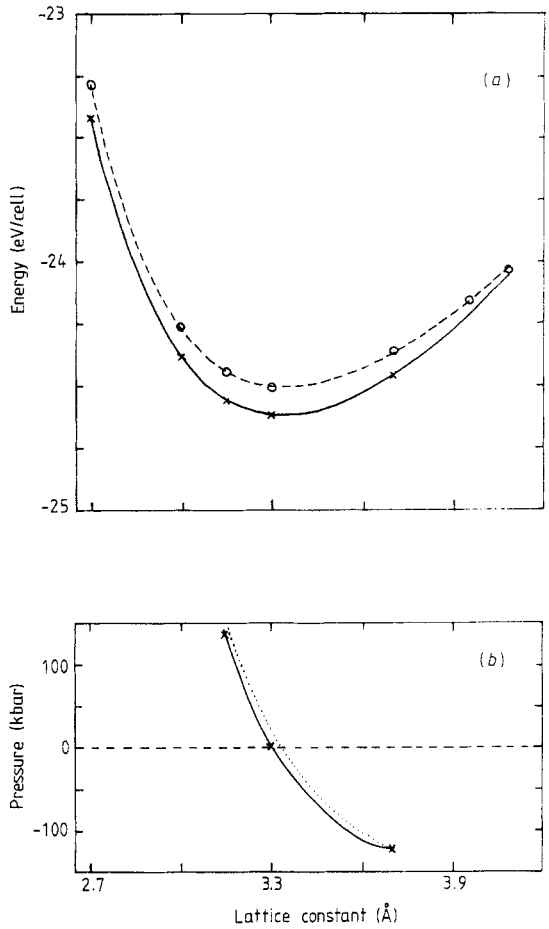


**Figure 1.** Equation of state of LiH (zero-point vibrations not included). (*a*) Energy $E^{LDA}$ calculated at different lattice constants within the LDA. With the plane-wave cut-offs 36 Ryd (– – –) and 60 Ryd (——) the position of the minimum, the second and third derivatives of $E^{LDA}$ are very little different. (*b*) Isotropic pressure calculated directly within the LDA scheme (——) compared with that obtained by differentiating the $E^{LDA}$ (*a*) above ($p = -\partial E/\partial V$) (· · · ·). Both curves correspond to the same plane-wave cut-off of 60 Ryd and their agreement indicates the degree of convergence: 1% difference in the position of equilibrium (the zero of $p(a)$).

**Table 1.** The convergence of the 'static equilibrium' evaluated at the minimum of the $E^{LDA}(V)$ (zero-point vibrations not included), assuming the Murnaghan equation of state (1). $E_2$ is the plane-wave cut-off, and the waves with kinetic energy between $E_1$ and $E_2$ were treated as the Löwdin perturbation; $l = 0$ was chosen as the 'local' component of the pseudopotential. The pressure $p(a_0)$ at 'static equilibrium' was evaluated directly within the DF scheme, using the 'stress theorem'; its closeness to zero indicates the degree of convergence of the energy calculations.

| $E_1$ (Ryd) | $E_2$ (Ryd) | Special points | $a_0$ (Å) | $B_0$ (Mbar) | $B_0'$ (—) | $p(a_0)$ (kbar) | $E^{LDA}$ (eV cell$^{-1}$) | Number of waves at $a_0$ |
|---|---|---|---|---|---|---|---|---|
| 12 | 12 | 2 | 3.32 | 0.68 | 4.05 | −110.3 | −24.1 | 80 |
| 12 | 12 | 10 | 3.45 | 0.55 | 2.55 | −97.7 | −23.8 | 84 |
| 12 | 12 | 28 | 3.43 | 0.57 | 3.57 | −86.4 | −23.8 | 86 |
| 36 | 36 | 10 | 3.35 | 0.59 | 3.83 | −28.7 | −24.5 | 424 |
| 48 | 60 | 10 | 3.34 | 0.66 | 3.57 | −11.3 | −24.2 | 905 |
| Experiment | | | 4.061 [24] | 0.31 [15] | 3.81 [15] | | | |

must be added the energy of the zero-point vibrations $\xi_0 = \sum \frac{1}{2}\hbar\omega_i$; the latter contribution is volume dependent as well, so that the static equilibrium (the minimum of $E^{\mathrm{LDA}}(V) + \xi_0(V)$) does not coincide with the minimum of $E^{\mathrm{LDA}}(V)$.

In most substances studied by the DF method so far, the contribution of $\xi_0(V)$ is small and can be neglected; in cases where this effect was considered (e.g. NaCl [35] or metallic Li [36]) the influence of $\xi_0$ is weak and the estimated correction to the lattice constants is of the order of 1%, always in the sense of expanding the lattice. In LiH, however, the zero-point vibrations can be expected to play a more important role than in crystals of heavier atoms; the order of magnitude of the shift in $a_0$ is not *a priori* clear.

In order to calculate the contribution of the zero-point motion precisely, complete knowledge of the vibrational spectrum is required. The phonon dispersion in LiH was measured [20] by inelastic neutron scattering, but detailed knowledge of the volume dependence of the phonon spectra is missing. An estimate of $\xi_0(V)$ can be attempted in terms of simple models: in a diatomic crystal, the energy per unit cell

$$\xi_0 \equiv \frac{1}{N}\sum_{i=1}^{6N} \tfrac{1}{2}\hbar\omega_i \tag{2}$$

can be evaluated in the Debye approximation as

$$\xi_0 = \tfrac{18}{8}\, k_{\mathrm{B}}\Theta_{\mathrm{D}} \tag{3a}$$

in agreement with the expression derived in [36] for a monatomic crystal. As the pressure variation is generally different for the acoustic and optic modes, we retain the Debye approximation only for the acoustic modes and deal with the optic modes separately, i.e. within the Einstein approximation; $\xi_0$ thus becomes

$$\xi_0 = \tfrac{9}{8}k_{\mathrm{B}}\Theta_{\mathrm{D}} + 3 \times \tfrac{1}{2}\hbar\omega(\mathrm{TO}(\Gamma)) \tag{3b}$$

or

$$\xi_0 = \tfrac{9}{8}k_{\mathrm{B}}\Theta_{\mathrm{D}} + 2 \times \tfrac{1}{2}\hbar\omega(\mathrm{TO}(\Gamma)) + \tfrac{1}{2}\hbar\omega(\mathrm{LO}(\Gamma)). \tag{3c}$$

To estimate the volume dependence $\xi_0(V)$ we assume, as in [36] that $k_{\mathrm{B}}\Theta_{\mathrm{D}}$ varies with volume as the square root of the bulk modulus $B$ and construct the $B(V)$ from the known values of $B_0$ and $B_0' = \mathrm{d}B(V)/\mathrm{d}p$ at $V_0$, assuming the (Murnaghan) equation of state. This leads to

$$\sqrt{B(V)/B(V_0)} = (V_0/V)^{B_0'/2}. \tag{4a}$$

The linearised form of this equation, for $V$ very little different from $V_0$, is

$$\sqrt{B(V)/B(V_0)} = 1 - (B_0'/2)[(V - V_0)/V_0] \tag{4b}$$

as was applied in [36]. The variation of the TO($\Gamma$) and LO($\Gamma$) eigenfrequencies with volume is described by the respective mode Grüneisen parameters $\gamma = -(\mathrm{d}\omega/\omega)/(\mathrm{d}V/V)$ which yields

$$\omega(V)/\omega(V_0) = (V/V_0)^{-\gamma} \tag{5a}$$

or, in the linearised form,

$$\omega(V) = \omega(V_0) - \omega(V_0)\gamma(V - V_0)/V_0. \tag{5b}$$

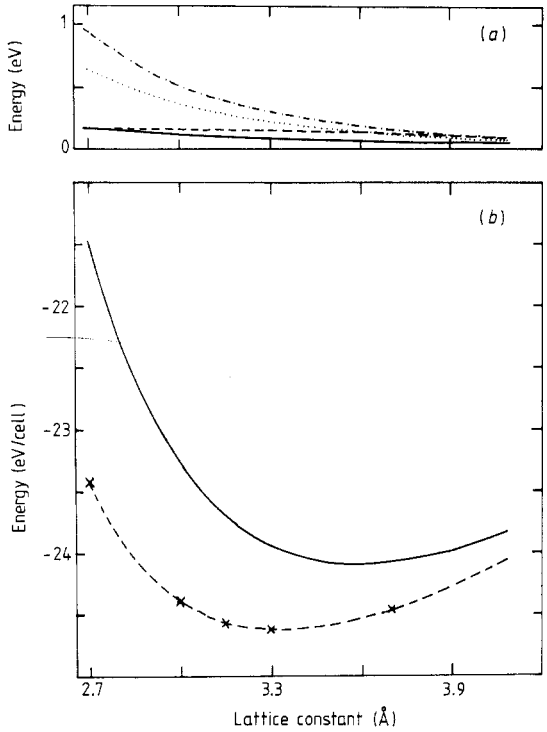


**Figure 2.** Zero-point vibrations in LiH and equation of state. (*a*) Different approximations for the zero-point energy $\xi_0$ and their variation with volume: —·—, Debye approximation $\frac{9}{8}k_B\Theta_D$ scaled as $\sqrt{B(a)}$, equation (4*a*); --- linearised form of the Debye approximation, equation (4*b*); ——, $\frac{1}{2}\hbar\omega(\text{TO}(\Gamma))$, taking for a Grüneisen parameter $\gamma = 1.2$; ····, $\frac{1}{2}\hbar\omega(\text{LO}(\Gamma))$, with $\gamma = 1.8$. (*b*) The total energy (——) obtained as the sum of $E^{\text{LDA}}$ (---) (identical with the full curve in figure 1(*a*)) and of $\xi_0$ given by equation (3*c*) (the chain, full and dotted curves in (*a*)). The inclusion of the zero-point vibrations shifts the static equilibrium by approximately 8% to the right; the corrected values of $a_0$, $B_0$ and $B_0'$ are given in table 2.

**Table 2.** Influence of the zero-point vibrations on the structural and static properties of LiH.

| | $a_0$ (Å) | $B_0$ (Mbar) | $B_0'$ (—) |
|---|---|---|---|
| Calculated from $E^{\text{LDA}}$ (*a*) curve in figure 1(*a*) | 3.34 | 0.66 | 3.57 |
| Corrected for zero-point motion | | | |
| Following equation (3*a*), assuming (4*a*) | 3.59 | 0.59 | 3.30 |
| Following equation (3*a*), assuming (4*b*) | 3.40 | 0.45 | 3.92 |
| Following equation (3*b*), assuming (4*a*) and (5*a*) | 3.54 | 0.57 | 3.30 |
| Following equation (3*c*), assuming (4*a*) and (5*a*) | 3.60 | 0.57 | 3.26 |
| Experiment | 4.061 [24] | 0.31 [15] | 3.81 [15] |

With the experimental values of $V_0$ [24], $\Theta = 920$ K [37], $B_0 = 0.3$ Mbar, $B_0' = 3.8$ [15], $\gamma(\text{TO}(\Gamma)) = 1.2$ and $\gamma(\text{LO}(\Gamma)) = 1.8$ [17], we obtain the volume variation in the terms in (3) shown in figure 2(*a*); the corrected equation of state which is shown in figure 2(*b*) leads to the prediction for $a_0$, $B_0$ and $B_0'$ summarised in table 2.

This way of taking into account the zero-point vibrations deserves some comments; with the corrections evaluated above, the assessment of the static equilibrium is no more truly *ab initio* because the experimental values have been used for $a_0$, $B_0$ and $B_0'$. However, the procedure could be accomplished without any experimental inputs—at least within the approximations (3)–(5)—because the TO($\Gamma$) frequencies can be calculated, at any given crystal volume, using the 'frozen-phonon' method [38]. The same

holds for $B(V)$; the bulk modulus can be evaluated from its definition at any $V$ using the calculated equation of state $E(V)$—be it in its 'uncorrected' version $E^{LDA}(V)$ or the 'corrected' form $E^{LDA}(V) + \xi_0(V)$. As the $\xi_0(V)$ depends on $B(V)$, it would be a matter of a few iterations to obtain $B(V)$ and $\xi_0(V)$ consistent with each other; the approximations (3)–(5) thus allow $\xi_0$ to be accounted for without any experimental input.

We can see from table 2 that the zero-point motion shifts the equilibrium lattice constant by at least 2%. The estimate, obviously, depends on the assumption which one adopts for the volume variation in $\xi_0$; however, all approximations which were not linearised (second, fourth and fifth rows in table 2) suggest a correction of between +6 and +8%. It is likely that, using equations (4*a*) and (5*a*) in order to describe the departures from the experimental equilibrium as large as 15% in lattice constant, one extrapolates the simple definitions (Grüneisen) and approximations (Murnaghan) beyond the interval on which they were measured or on which their validity can be relied upon. The correction of +8% to $a_0$ suggested by the fifth row in table 2 should thus be considered as the upper limit for the estimate of the influence of the zero-point motion. This implies that the present disagreement between the calculated equilibrium and the experimental must be caused by other reasons that the zero-point motion; they will be discussed in § 4.

## 3. Electronic properties

### *3.1. Charge densities*

The calculated charge (pseudo-charge) density and its real-space distribution are shown in figures 3, 4 and 5. It can be seen in figure 3(*a*), which is a linear plot along the cube edge, that nearly all electrons are piled up on the H atom, the Li core is surrounded by very little charge. When pressure is applied, the shape of the distribution is almost unaltered but a part of the charge is transferred into the rare 'empty' space left, which still exists near the centre of the Li–H cube diagonal (see figure 3(*b*)) and in the middle of the second-neighbour Li–Li and H–H 'bonds' (see figures 3(*c*) and 3(*d*)). The contour plots in figures 4 and 5 give the distribution in the (100) and (111) planes, at the lattice constant $a = 3.7$ Å, which is our calculation nearest to the predicted static equilibrium ($a = 3.60$ Å). It can be inferred from these plots that the essential part of the charge is spherically distributed around the H sites (figures 4(*a*) and 5(*a*)), illustrating the idea of a nearly perfect ionic bonding. The remaining charge is distributed over the rest of the volume and only the plots giving the low-density part of the distribution (figures 4(*b*), 5(*b*) and 5(*d*)) show any departures from the spherical distribution. These conspicuous departures from the spherical shape amount, however, to fairly little; for example, on a sphere around Li with the radius 0.19*a* (about 40% of the Li–H distance; see figure 4(*b*)), charge varies between 0.9 and 1.2 electrons cell$^{-1}$. The H ion is also only slightly aspherical, and only in the low-density region; for example, the radius of the last closed contour around H ($n(r) = 1.3$ electrons cell$^{-1}$; see figure 4(*b*)) varies from 0.30*a* to 0.33*a*. In the high-density region (contours of 2 electrons cell$^{-1}$ or more) the distribution is perfectly spherical. Under compression, figures 4(*a*) and 5(*a*) remain essentially unchanged—although labelling of the contours would be modified, as can be inferred from figure 3—and the low-density contours around Li (figure 4(*b*)) become even more aspherical, because the charge keeps filling the space between the second neighbours.

Qualitatively, figure 3 allows us to conclude that most of the electronic charge is transferred from Li to H. Any more exact and quantitative statement will depend on

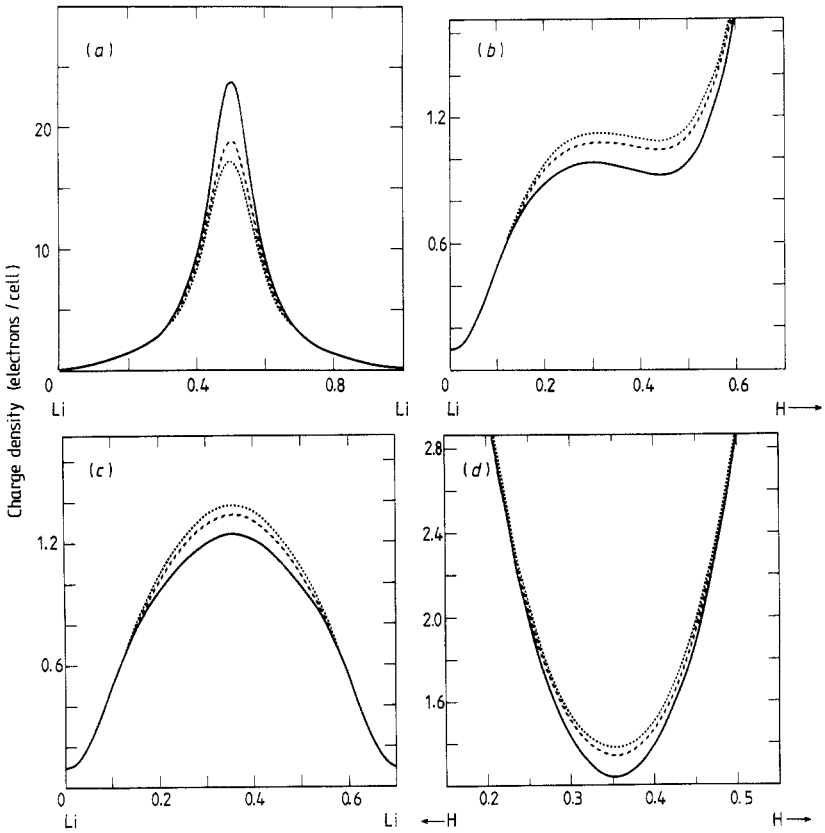


**Figure 3.** Variation is the pseudo-charge density of LiH along (*a*) [100] (the cube edge), (*b*) [111] (the cube main diagonal) and (*c*) [110] and (*d*) the effect of hydrostatic pressure: ——, 3.7 Å; – – –, 3.3 Å; · · · ·, 3.5 Å. The unit of length is the lattice constant *a*, and the unit cell volume is $a^3/4$.

the criterion which we choose for defining the H or the Li region. The simplest and unambiguous way is to divide space into equal cubes of side $a/2$ and having the H or Li atom in the centre. The cubes fill the space entirely and an integration of the charge density over the cubic regions gives for the (pseudo-)charge 1.46 electrons around H and 0.54 electrons around Li. There is good agreement between these numbers and the experimental value of 1.52 electrons in the H cube obtained in [16] from x-ray measurements.

The main advantage of the cubic regions is in their unambiguous definition and in the possibility of comparing the integrated charge with the experimental data. It is nevertheless preferrable (although more subjective) to have a definition of the H and Li regions which reflects the actual shape of the charge distribution and which is closer to the spheres than to the cubes. Taking the largest closed contours around H and Li, we can consider the charge inside them as belonging to H or Li; these are contours 1.3 and 1.2, respectively (see figure 4(*b*)). Simplifying the geometry slightly, we integrate $n(\boldsymbol{r})$ over the spheres with radii $0.303a$ and $0.197a$ which gives a pseudo-charge of 1.45 electrons on H and 0.10 electrons on Li; the remaining charge of 0.45 electrons is distributed in the interstitial region. This way of assigning charge to spheres rather than inside the contours leads to a small underestimation of both the H and Li charges, i.e. to an overestimate of the amount of charge in the interstitial region. It seems somewhat

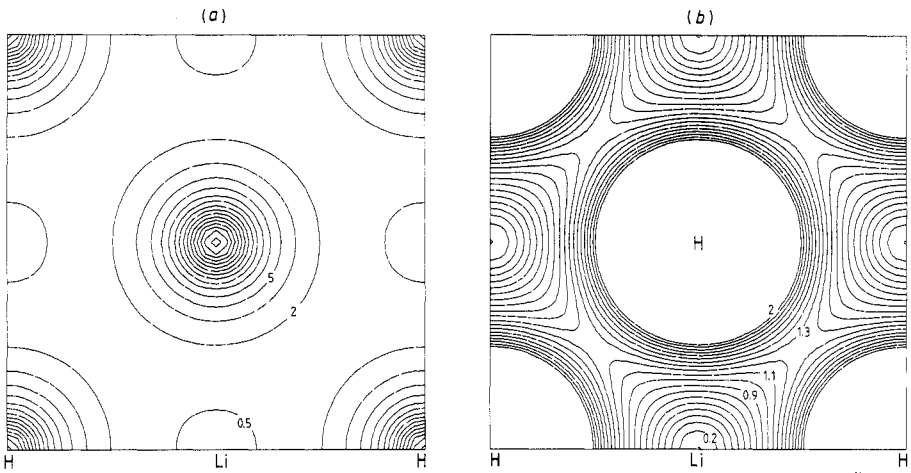


**Figure 4.** Contour plots of the pseudo-charge density in the plane (100), at $a = 3.7$ Å (i.e. close to the calculated equilibrium). The H atoms are in the centre and at the corners of the square; the Li atoms are at the sides. (*a*) The essential part of the electronic charge is spherically distributed around the H sites. The small square contours in the centre are due to the finite size of the mesh used. (*b*) Plot complementary to (*a*), displaying the low-density details of the $n(\boldsymbol{r})$ ($\leqslant 2.0$ electrons cell$^{-1}$) which could not be resolved in the scale of (*a*). Units of $n(\boldsymbol{r})$ are the same as in figure 3; the contour interval is 1.5 electrons cell$^{-1}$ in (*a*) and 0.1 electron cell$^{-1}$ in (*b*).

surprising that the H charge is nearly the same, whether integrated over the cube or over the sphere, but inspection of figure 4(*b*) reveals that a cube of side $a/2$ around the H occupies roughly the same space as the sphere. For comparison, the APW calculations in [9] using muffin-tin spheres with radii $0.262a$ and $0.238a$ accumulated charges of 1.13 electrons around H and 0.259 electrons (plus 2 electrons from the core) around Li.

All integrations above were performed at 3.7 Å, i.e. close to the calculated equilibrium. Under compression, the charge in the 'H volume' is reduced—although much less than the volume itself; with $a$ reduced from 3.7 to 3.3 Å, in the H cube the charge decreases from 1.46 to 1.43 electrons, in the H sphere it increases from 1.45 to 1.36 electrons and in the Li sphere it increases from 0.10 to 0.12 electrons. In dealing with pressure variations, it is the idea of the 'last closed contour' that we maintain under compression: the sphere radii become $0.297a$ and $0.203a$, respectively.

The above values should not be given more significance than they really have. All integrations are very sensitive to the choice of the sphere radius $R$ and the departures of $n(\boldsymbol{r})$ from sphericity were not taken into account. It should also be stressed that the static charges discussed here are not to be confounded with the effective charges which bring about the LO–TO($\Gamma$) split in the phonon spectra.

### *3.2. Band structure*

Although the DF eigenvalues are known to underestimate the gaps, we have plotted in figure 6 the band structure of LiH, in order to provide a reference and to compare with other schemes; consistently with the charge densities in figures 4 and 5 the $\varepsilon_i(\boldsymbol{k})$ were evaluated at $a = 3.7$ Å, i.e. close to the calculated equilibrium. The overall 'topology' of figure 6 agrees well with other band-structure calculations [6–10]. The minimum gap (2.14 eV) situated at X is certainly a strongly underestimated consequence of the LDA. Let us remember that the Hartree–Fock calculations in [6] and [7] (expected to overestimate the gaps) obtained, respectively, 14.5 and 10.5 eV; with correlation incorporated approximately into the Hartree–Fock scheme in [8], the gap became 6.61 eV.

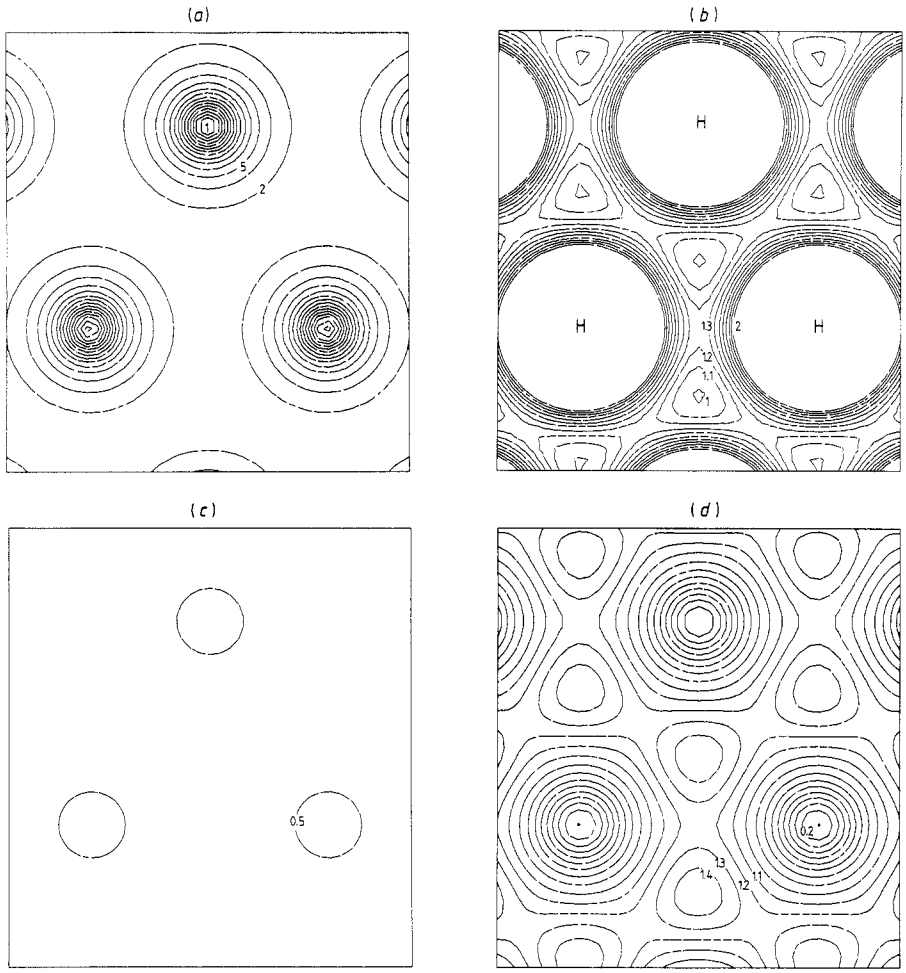


**Figure 5.** Contour plots of pseudo-charge density in the plane (111), at $a = 3.7$ Å. (*a*), (*b*) The plane contains only H atoms located at the centres of the nearly spherical contours: (*a*) plot displaying the high density of $n(\boldsymbol{r})$ ($\geqslant 2$ electrons cell$^{-1}$); (*b*) same as in figure 4(*b*). (*c*), (*d*) Same as (*a*), (*b*) but for the (111) plane containing only Li atoms located at the centre of the nearly spherical contours.

Our present value is consistent with the value of 2.31 eV obtained in [9], using the same LDA approximation within the APW scheme. No experimental data are available for comparison—not in the published literature, at least. The LDA and Hartree–Fock results are likely to be the lower and upper bounds to reality.

## 4. Discussion

Some of the results shown in § 3 are pertinent to static equilibrium; in the absence of better agreement with experiment, it is the calculations close to the predicted equilibrium ($a = 3.6$ Å) which are the most likely to describe reality at zero pressure. We verified this by a few orientational calculations of the TO($\Gamma$) frozen phonon at different pressures, and the band-structure calculations performed in [9] at different pressures support the

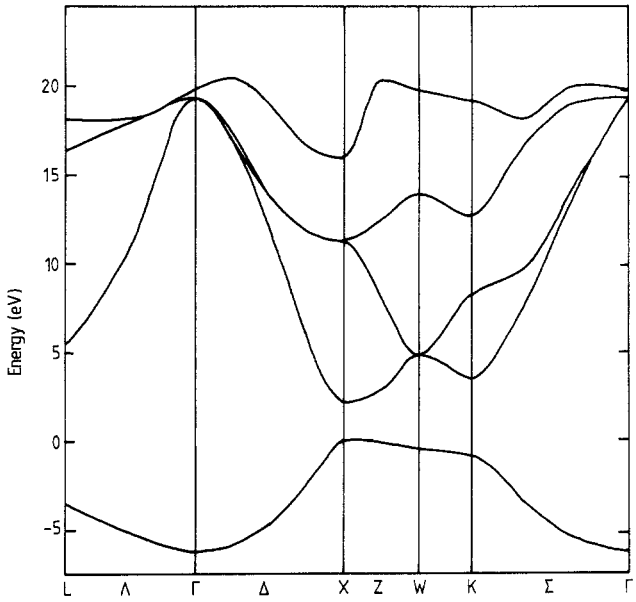


**Figure 6.** Band structure of LiH calculated within the LDA at $a = 3.7$ Å (near the predicted equilibrium). The gap obtained at X is 2.14 eV.

same idea. The question is what are the probable reasons for the approximately 10% error in $a_0$, larger than is usual in this type of calculation. The zero-point vibrations $\xi_0(V)$ have already been eliminated above; they are not the main reason for the disagreement. One can still question the form of the DF and the pseudopotential.

The present calculations were performed with the Ceperley–Alder exchange and with the $l = 0$ pseudopotential selected as the local component. A few orientational calculations done at lower cut-offs revealed that using the Wigner formula for exchange–correlation moves the calculated minima imperceptibly (towards larger $a$). Using for H the full Coulomb potential moves the position of minimum also very little (towards smaller $a$). Choosing a different component of the pseudopotential as the local one ($l = 2$ for Li and H) shifts the position of minimum by about 5% towards still lower values of $a$. Using the $V^{\text{core}}$ in [29] as the local component does not give any substantial improvement, either.

We carefully examined whether the discrepancy could be caused by the large spatial extent of the d wavefunctions in both Li and H. In fact, the cut-off radii $r_{\text{cl}}$ actually used for generating the $l = 2$ components of the pseudopotentials in [29] sum [39] to 4.8 au, which is 25% more than the observed Li–H spacing at equilibrium. This means that the d contributions to the wavefunctions overlap already in the 'pseudised' regions, where the pseudopotential description does not apply. As it has been verified [39] that the Li pseudopotential in [29] without the d component and the H pseudopotential with only the s component reproduce the atomic states of the Li and H atoms in many excited configurations as successfully as the 'complete' pseudopotentials, we carried out the structural determination on LiH also with these pseudopotentials. As a result, one obtains a slight improvement in the bulk modulus (by about −0.1 Mbar) but the lattice constant does not change by more than +0.02%, which demonstrates the relatively small importance of the d contributions to the wavefunctions. The suitability of employing the full Coulomb potential for H was rechecked in this context, as well. In all these

verifications the $V^{core}$ in [29] was chosen as the 'local' component; the two special points used for sampling and the energy cut-off were gradually increased up to 72 Ryd (without the Löwdin perturbation)—which allowed us to confirm once more that the 60 Ryd cut-off is sufficient for obtaining converged structural and static properties†.

The problem of the approximately 10% discrepancy in the lattice constant thus remains to a large extent unexplained. The main cause of disagreement is not the LDA itself because systems such as metallic Li [36] or even solid H [40] have been successfully described within this approximation. After the pseudopotential, one can still question the rigid-core approximation underlying the use of any pseudopotential; this assumption may be inadquate in Li.

## 5. Conclusion

The DF theory was used to study the structural and static properties of LiH from first principles; the role of zero-point vibrations was discussed and different estimates for the volume variations of this contribution were proposed and compared. The real-space distribution of electronic charge density was studied in detail; contour plots in selected planes and pressure variation in the charge along the principal symmetry directions were given. The calculations revealed a spherical charge distribution typical of ionic bonding and a strong charge transfer from Li to H. Integration of charge density was attempted, with the aim of assigning definite values of charge to the individual atoms and comparing with the same quantities determined from x-ray measurements. The reason for the 10% disagreement between the calculated and experimental lattice constant could not be conclusively identified; several plausible causes were examined and had to be rejected. Finally the DF band structure of LiH is calculated and compared with previous determinations within the Hartree–Fock scheme.

## Acknowledgments

We wish to express our thanks to G Vidal-Valat and J P Vidal for bringing to our attention the problem of charge density in LiH. We are grateful to G B Bachelet for pointing out the size of the Li wavefunctions, as well as for verifying for us the excited states of the Li and H pseudo-atoms. We have benefited from discussions with B Alder, M Besson, O H Nielsen, R Pick and R Zeyher. One of us (COR) thanks the French Ministry of Foreign Affairs and the Argentine Secretaría de Ciencia y Técnica for financial support. This work was partly supported by a NATO grant and the computer resources were provided by the Scientific Committee of Centre de Calcul Vectoriel pour la Recherche, Palaiseau, France.

*Note added in proof.* The band gap of LiH was recently determined experimentally [41] to be 4.94 eV. After the present work was completed, results of theoretical studies of the equation of state and the B1–B2 transition by the APW method have been published [42]. Also, it has been shown [43] that converged results can be obtained with plane waves when the full, unscreened Coulomb potentials are used for both Li and H (i.e. $+3/r$ and $+1/r$ instead of pseudopotential); a good agreement of the ground-state properties with experiment is obtained in this way ($a_0 = 3.9$ Å, when the zero-point vibration term is not included).

## References

[1] Hylleras E A 1930 *Z. Phys.* **63** 771
[2] Ewing D H and Seitz F 1936 *Phys. Rev.* **50** 760

† The 60 Ryd results for $a_0$, $B_0$ and $B_0'$ are 'stable' to within 0.1% in $a_0$, 1.6% in $B_0$ and 3.3% in $B_0'$.

[3] Löwdin P O 1956 *Adv. Phys.* **5** (17) 1
[4] Morita A and Takahashi K 1958 *Prog. Theor. Phys.* **19** 257
[5] Lundqvist S O 1954 *Ark. Fys.* **8** 177
[6] Kunz A B and Mikish D J 1973 *J. Phys. C: Solid State Phys.* **6** L83
[7] Dovesi R, Ermondi C, Ferrero E, Pisani C and Roetti C 1984 *Phys. Rev.* B **29** 3591
[8] Kunz A B and Mikish D J 1975 *Phys. Rev.* B **11** 1700
[9] Perrot F 1976 *Phys. Status Solidi* b **77** 517
[10] Baroni S, Pastori Parravicini G and Pezzica G 1985 *Phys. Rev.* B **32** 4077
[11] Berggren K F 1969 *J. Phys. C: Solid State Phys.* **2** 802
[12] Kulikov N I 1978 *Sov. Phys.–Solid State* **20** 1170
[13] Hammerberg J 1978 *J. Phys. Chem. Solids* **39** 617
[14] Bashkin I O, Dymova T N and Ponyatovskii E G 1980 *Phys. Status Solidi* b **100** 87
[15] Gerlich D and Smith C S 1974 *J. Phys. Chem. Solids* **35** 1587
[16] Calder R S, Cochran W, Griffiths D and Lowde R D 1962 *J. Phys. Chem. Solids* **23** 621
[17] Vacher R, Boissier M and Laplaze D 1981 *Solid State Commun.* **37** 533
[18] Laplaze D 1979 *Phys. Status Solidi* b **91** 59
[19] Benedek G 1967 *Solid State Commun.* **5** 101
[20] Verble J L, Warren J L and Yarnell J L 1968 *Phys. Rev.* **168** 980
[21] Jaswal S S and Hardy J R 1968 *Phys. Rev.* **171** 1090
[22] Zeyher R 1975 *Phys. Rev. Lett.* **35** 174
[23] Grosso G, Pastori Paravicini G and Resta R 1976 *Phys. Status Solidi* b **73** 371
[24] Vidal J P and Vidal-Valat G 1986 *Acta Crystallogr* B **42** 131
[25] Vidal-Valat G and Vidal J P 1985 *8th Sagamore Conf. on Charge, Spin and Momentum Density (Sanga-Saby) 28 July–3 August 1985*; 1986 *Chem. Scr.* **26** 479
[26] Loupias G and Chomilier J 1986 *Z. Phys.* D **2** 297
[27] Rodriguez C O and Kunc K 1987 *Solid State Commun.* **64** 19
[28] Hohenberg P and Kohn W 1964 *Phys. Rev.* B **136** 864
Kohn W and Sham L J 1965 *Phys. Rev.* A **140** 1133
Sham L J and Kohn W 1966 *Phys. Rev.* B **145** 561
[29] Bachelet G B, Hamann D R and Schlüter M 1982 *Phys. Rev.* B **26** 4199
[30] Ceperley D M and Alder B J 1980 *Phys. Rev. Lett.* **45** 566
[31] Ihm J, Zunger A and Cohen M L 1979 *J. Phys. C: Solid State Phys.* **12** 4409
[32] Nielsen O H and Martin R M 1983 *Phys. Rev. Lett.* **50** 697
[33] Murnaghan F D 1944 *Proc. Natl. Acad. Sci. USA* **30** 244
[34] Gomes Dacosta P, Nielsen O H and Kunc K 1986 *J. Phys. C: Solid State Phys.* **19** 3163
[35] Froyen S and Cohen M L 1984 *Phys. Rev.* B **29** 3770
[36] Dacorogna M M and Cohen M L 1986 *Phys. Rev.* B **34** 4996
[37] Pretzel F E, Rupert G N, Mader C L, Storms E K, Gritton G V and Rushing C C 1960 *J. Phys. Chem. Solids* **16** 10
[38] Kunc K and Martin R M 1981 *Phys. Rev.* B **24** 2311
[39] Bachelet G B 1987 private communication
[40] Min B I, Jansen H J F and Freeman A J 1986 *Phys. Rev.* **33** 6383
[41] Kondo Y and Asaumi K 1988 *J. Phys. Soc. Japan* **57** 367
[42] Hama J and Kawasami N 1988 *Phys. Lett.* A **126** 348; and private communication
[43] Kunc K 1989 *Proc. Int. Conf. Applications of the Density Functional Theory to Chemical and Physical Properties of Inorganic Systems (Arles, France 1988)* at press